JOURNAL OF CATALYSIS **159,** 204–211 (1996)
ARTICLE NO. 0079

High-Temperature, High-Pressure *in Situ* Reaction Monitoring of Heterogeneous Catalytic Processes under Supercritical Conditions by CIR-FTIR

Zissis Dardas, Murat G. Süer, Yi H. Ma, and William R. Moser

Department of Chemical Engineering, Worcester Polytechnic Institute, Worcester, Massachusetts 01609

Received May 3, 1995; revised November 1, 1995; accepted December 11, 1995

An *in situ* cylindrical internal reflection infrared technique (CIR-FTIR) was developed, which permits the real time analysis of supercritical fluids and heterogeneous catalytic processes at temperatures up to 500°C and 1000 psi pressure (1 psi = 6850 Pa). High-quality spectra were obtained at both high temperatures and high pressures under *in situ* reaction conditions.

The molecular thermal transitions that a hydrocarbon undergoes in the supercritical regime, the properties of a hydrocarbon within the pores of a zeolite, and the interactions of a hydrocarbon with the active acid sites of the zeolite during catalytic cracking were studied by this technique. The results showed that the stretching frequency of the C–H bonds was altered in supercritical heptane, probably due to intermolecular hydrogen bonding. IR data also demonstrated an increased heptane concentration within the micropores of a commercial catalytic cracking, Y-type zeolite (promoted Octacat) during catalytic cracking at supercritical conditions. This method also enabled a determination of the types of hydroxyl groups contained within the zeolite (i.e., Brønsted acid sites in the supercages and sodalite cages, terminal silanols, and superacid sites) and their relative concentration changes with increasing temperature. Finally, the alteration of the concentrations of the various catalytic active sites together with the appearance of new bands was also monitored *in situ* during catalytic cracking of heptane at 475°C under subcritical and supercritical conditions. © 1996 Academic Press, Inc.

INTRODUCTION

The main problem in the analysis of heterogeneous catalytic reaction systems by transmission or diffuse reflectance infrared is that the gas-phase reactant is usually strongly absorbing in the same region of the spectrum as the surface adsorbed species of mechanistic interest (chemisorbed adsorbates). This problem is greater in the *in situ* analysis of systems at high pressures since the high gas concentrations together with the long path lengths give rise to intense gas-phase absorption bands making their subtraction from the *in situ* spectra unreliable (1). The unique advantage of the cylindrical internal reflectance IR (CIR-IR) technique in the study of heterogeneous catalytic reaction systems is that the IR beam mainly samples the solid catalyst and chemisorbed molecules. Since the CIR method is also a short path length technique, the IR spectra is not dominated by the presence of strongly absorbing gas-phase bands even at high pressures. Therefore, this method permits the reliable and quantitative computer subtraction of high-pressure gas-phase bands from the region in which the adsorbate appears in the infrared. This improvement is significant as compared to previous research studies using transmittance cells of diffuse reflectance cells, where the IR beam path length through the gas phase is large relative to that through the catalyst sample.

The CIR-IR technique offers an important advantage in the analysis of powdered catalyst samples. In the case of transmission IR techniques the solid catalyst sample must be pressed to very high pressures in order to form a thin wafer. This may collapse the pores of the catalyst and complicate the IR analysis due to the diffusion limitation of the reacting gas or fluid into the interior of the catalyst. The advantage of the CIR-IR technique is that it can be used on powders for the *in situ* analysis of chemical reaction systems when mounted in the appropriate reactor cells. A high-pressure, plug flow microreactor, equipped with an embedded CIR crystal and high temperature seals, was developed in this study for the *in situ* reaction monitoring of heterogeneous catalytic processes. The focus of this paper is to demonstrate the capabilities of the CIR-reactor technique for both high-temperature and high-pressure *in situ* monitoring. The capabilities of this method for the *in situ* heterogeneous catalysis monitoring will be examined using supercritical heptane cracking over a Y-type zeolite.

The basic principles involved in the CIR technique are depicted in Fig. 1. An incident IR beam strikes the internal reflection element (a polished cylindrical crystal), propagates in the crystal, and undergoes total internal reflection at the interface with the sample under study, when the incidence angle θ (which is measured from the normal) exceeds the critical angle θ_c (2). In this case, the incident IR radiation creates a standing, evanescent electromagnetic wave just at

0021-9517/96 $18.00

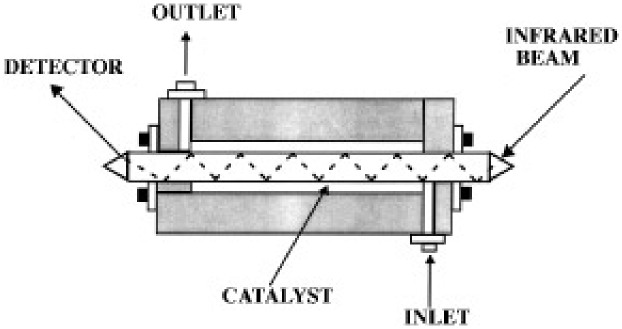

FIG. 1. Schematic of the CIR heterogeneous reactor, illustrating also the principles of the CIR-IR technique.

the interface penetrating into the sample. The penetration depth of this wave is given by the following expression (2):

$$d_p = \frac{\lambda/n_1}{2\pi(\sin^2\theta - (n_2/n_1)^2)^{0.5}} \qquad [1]$$

where n_2 and n_1 are the refractive indices of the medium under study and of the crystal, respectively, and λ is the wavelength of the IR radiation. The number of internal reflections through the length of the crystal is equal to $(L/D)\cot\theta$, where L is the length and D is the diameter of the crystal (2).

The principle of this technique was discovered nearly two centuries ago by Newton. However, it was not developed for the production of absorption spectra until the pioneering work of Harrick (3, 4) and Fahrenfort (15). The application of the CIR technique to chemical process analysis was first introduced by Wilks and co-workers (6). The optical and mechanical design of the optical bench required for laboratory IR analysis was invented and developed by Sting and Wilks (7).

Techniques previously described in the literature for high-pressure *in situ* reaction monitoring of homogeneous metal-catalyzed reactions by IR spectroscopy were mainly based on transmission IR cells (8–11). The CIR technique was successfully applied by Moser and co-workers (12–16) to the development of high-pressure/high-temperature well-stirred liquid-phase autoclaves (CIR-reactors). These reactors enabled them to monitor *in situ* the progress of homogeneous catalyzed reaction systems and to identify and measure the concentration of active intermediate species. The most recent development in the technology uses optical fiber CIR coupled high-pressure reactors to achieve remote sensing (17). Prior CIR-reactor studies in our lab with the stirred batch reactor demonstrated that high-quality spectra could be obtained at high pressures near 1500 psi when studied to moderate temperatures up to 150°C (18). Studies in the solids reaction cell showed that good quality spectra could be obtained at temperatures up to 420°C but at pressures slightly above atmospheric. Yokoyama et al. (19), obtained absorption spectra of supercritical CO_2 at 40°C and high pressures in a specially designed high-pressure CIR cell. Most recently, Jolly *et al.* (20) studied the catalytic cracking of *n*-hexane on dealuminated H−Y zeolites by using *in-situ* transmission IR spectroscopy up to temperatures of 400°C but at atmospheric pressure.

To date, no work has been reported in the literature on CIR infrared analysis at both high temperatures and high pressures. Therefore, the objective of this study was to demonstrate that infrared spectra of very high quality could be obtained by use of the CIR-FTIR technique at temperatures as high as 500°C and pressures up to 1000 psi (1 psi = 6850 Pa). Current studies in our laboratory are focused on obtaining *in situ* information on the mechanisms of hydrocarbon catalytic cracking under supercritical conditions in order to understand the stability of the zeolitic catalyst toward rapid deactivation.

EXPERIMENTAL

Figure 1 illustrates the heterogeneous CIR plug flow stainless steel microreactor used in this study. The optical rod embedded in the reactor was a ZnSe crystal, 0.25 in. in diameter and 3.25 in. long, with conical ends, and polished at 45° to the axis. The cut-off frequency of ZnSe is 670 cm^{-1}. This crystal has the mechanical strength to withstand the high stresses induced by the high pressures and temperatures employed in the experiment. The crystal was effectively sealed in the reactor using graphite O-rings. A thin gold layer was deposited onto the seal rings to prevent absorption of the IR beam at the seal/crystal contacting areas by the strongly absorbing graphite. The incoming IR beam was directed to a set of focusing mirrors where the beam was directed at a 90° angle on to the conical ends. As the beam passes through the crystal, it undergoes 13 internal reflections at the interface of the crystal with the surrounding medium before it exits the crystal and is redirected toward the detector by another set of mirrors. The quality of catalyst to crystal contact determines the quality of the CIR-IR spectra, especially at high temperatures where the crystal loses much of its optical transparency. As the catalyst particle size decreases, the contact to the crystal increases and the quality of the spectra increases. Experimentally we have found using several different materials that particles within the 10 to 40 μm range result in high spectra quality.

CIR crystals lose a high percentage of their optical transparency at temperatures higher than 300°. We determined that the ZnSe crystal behaves substantially better at high temperatures than the Si crystal. Part of this behavior is due to the fact that the Si crystal quickly loses its optical transparency at high temperatures. In addition, the penetration depth using a Si crystal polished at 30°C to the axis is inherently less. Since the average refractive index for Si is 3.50, for ZnSe is 2.40, and for heptane is 1.43, it was calculated using Eq. [1] that the penetration depth in the surrounding heptane with a ZnSe crystal is 2.2 times higher than that of an Si crystal. The difference in the penetration depths between these two crystals is even larger for the case of the solid material (zeolite). Since the refractive index for the zeolite is 1.6, the penetration depth in the zeolite with the ZnSe crystal is 3.3 times higher than that with the Si crystal at any wavelength. The penetration depth in the zeolite using the ZnSe crystal changes from 0.24 to 0.82 μm for wavenumbers between 4000 and 670 cm^{-1}.

A midrange infrared spectrometer (Nicolet 510P), continuously purged with nitrogen and equipped with an Mercury Cadmium Telluride-B detector, was used to acquire all IR spectra. The IR spectra were collected at a spectral resolution of 4 cm^{-1} by co-adding 1024 scans to obtain the desired signal to noise ratio unless otherwise specified. This gave an acquisition time of roughly 10 min for each spectrum. The supplied Nicolet software was used for spectral manipulation (ratioed to background, baseline subtraction and smoothing). However, spectral deconvolution was performed using a Galactic Software, Grams 386 program.

A schematic of the experimental apparatus used in these studies is shown in Fig. 2. The high-pressure CIR-microreactor was mounted in the sample compartment of the FT-IR spectrometer. The cell was encapsulated within a cubic, insulated, copper alloy block, heated by four Omega cartridge heaters. The reactor temperature was measured with a K-type thermocouple and controlled with an Omega temperature controller. The CIR-cell/heating block system was mounted on a Spectra-Tech CIRCLE optical bench. A precision metering, high-pressure, low-volume pump was used for liquid circulation. Other facilities included high-pressure inlet and outlet 1/16 in. lines, a by-pass line to fill-up the system with liquid without going through the reactor, a down-stream back pressure regulator, pressure gauges, and mass flow meters. Pressure was measured at the pump and at the exit of the reactor. Temperature measurement of the stream 1.5 in. after the exit of the reactor showed a 60°C difference from the reactor temperature. The line after the back pressure regulator was heat traced for on-line GC analysis. The system was purged with flowing nitrogen before and after each experiment.

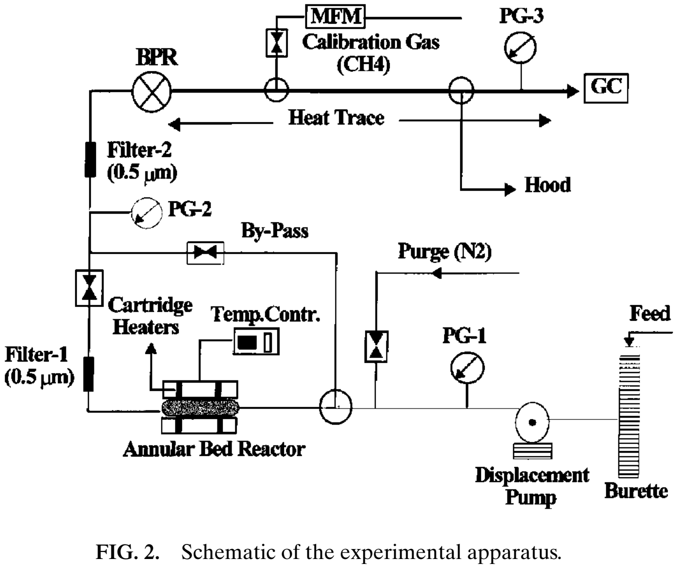

FIG. 2. Schematic of the experimental apparatus.

CIR crystals were purchased from Spectral Systems while the hydrocarbons (heptane, etc.) of 99% purity were obtained from Aldrich. The catalyst samples (promoted Octacat, a commercial catalytic cracking H–Y type zeolite) were supplied from Davison–Grace Chemicals and had the following composition:

- 27 wt% of dealuminated (ultra-stable) H–Y zeolite with Si/Al = 9. This zeolite contained 0.4 wt% Na$_2$O and no rare earths.
- 3 wt% H-ZSM-5 with Si/Al = 25, no rare earths, and Na$_2$O less than 0.1 wt%.
- The remaining 70 wt% was the "dilution" matrix, which mainly consisted of kaolinite clays (90% by weight). The balance was silica, which serves as a binder and amorphous aluminum phosphates.

All samples were calcined at 450°C for 8 h prior to each experiment.

RESULTS AND DISCUSSION

In Situ CIR-IR Characterization of Heptane and of Heptane over Zeolite at High Temperatures and Pressures

The *in situ* IR absorbance spectra of the C–H stretching modes of heptane flowing in an empty cell at subcritical (200°C) and supercritical conditions (above 325°C), are shown in Fig. 3. The critical conditions for heptane are $T_\mathrm{c} = 267$°C and $P_\mathrm{c} = 397$ psi. Each of these spectra resulted from the co-addition of 256 scans, corresponding to an acquisition time of 2.5 min. The pressure in this experiment was held at 500 psi (1 psi = 6850 Pa), i.e., 100 psi above the critical pressure. Figure 3 illustrates the high-quality spectra which were obtained using the CIR technique at high temperatures and substantially higher pressures than previously employed. Furthermore, this figure demonstrates that just as the critical temperature was reached, the IR stretching frequencies substantially broadened. This broadening of the spectra that characterize the supercritical state is also illustrated in the curve-fitted spectra, shown in Fig. 4. Spectra deconvolution showed a 40% increase in the full width at half maximum (FWHM) of the peak at 2965 cm^{-1} at supercritical conditions and a 16% increase in the width of the 2930 cm^{-1} peak. These figures suggest that the hydrocarbon molecules undergo an alteration of the C–H stretching bonds in the supercritical regime and the CIR-IR technique

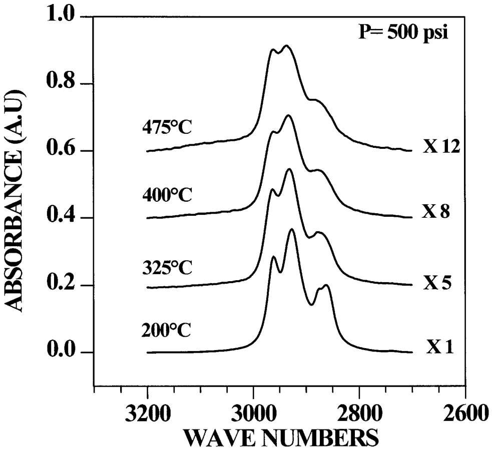

FIG. 3. *In situ* CIR-IR spectra of the stretching C–H modes of heptane flowing in an empty CIR-IR cell at subcritical (200°C) and supercritical conditions (325°C and above). Heptane pressure, 500 psi (1 psi = 6850 Pa), LHSV = 100 h^{-1}. Critical conditions of heptane, $P_c = 397$ psi, $T_c = 267$°C.

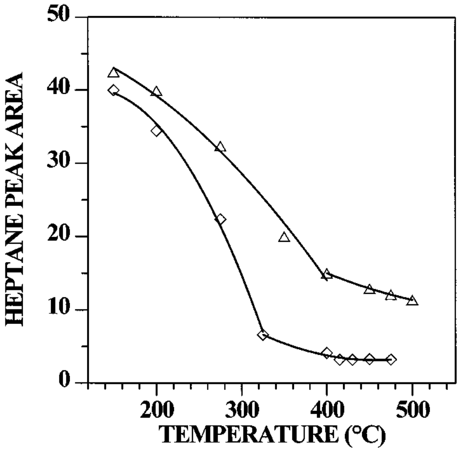

FIG. 5. The heptane integrated absorbance peak area vs temperature for heptane flowing in an empty CIR-IR cell (lower curve) and for heptane flowing in the CIR-IR cell packed with promoted Octacat (upper curve). For both experiments, heptane pressure, 500 psi, LHSV = 100 h^{-1}.

is capable of continuously monitoring these bond modifications. The alteration in the C–H stretching frequency is attributed to the increased solvent–solvent intermolecular interactions in the supercritical fuel (a well-known phenomenon called clustering (21), possibly due to intermolecular hydrogen bonding.

The pure heptane integrated absorbance peak area vs temperature is shown in Fig. 5 (lower curve). This figure indicates that while the IR signal gradually dropped in intensity as the temperature increases over the range that corresponds to the subcritical regime, it abruptly dropped in intensity just at the critical temperature. After that, it practically remained constant over the broad temperature range that corresponds to the supercritical regime (i.e., from temperatures between 270 and 475°C). A major part of this behavior is caused by the sudden change in the refractive index of the hydrocarbon at the critical point which consequently decreases the penetration depth of the IR radiation in the heptane. Similar results to those presented in the previous two figures were obtained with the well-stirred CIR autoclave, which has been used to study the supercritical state of more than 10 different hydrocarbons and hydrocarbon mixtures (22).

The high-quality *in situ* IR spectra of heptane flowing through the catalyst (promoted Octacat) during cracking under subcritical (200°C, 500 psi, liquid phase) and supercritical conditions (500 psi, temperature 325°C and above) are shown in Fig. 6. Figure 5 (upper curve) illustrates the changes in the integrated absorbance area as a function of temperature for these spectra. The first surprising

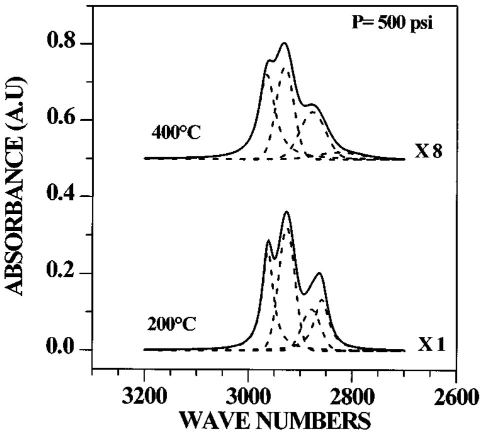

FIG. 4. Curve fitting of a subcritical (200°C) and a supercritical (400°C) heptane spectrum. Heptane pressure, 500 psi, LHSV = 100 h^{-1}.

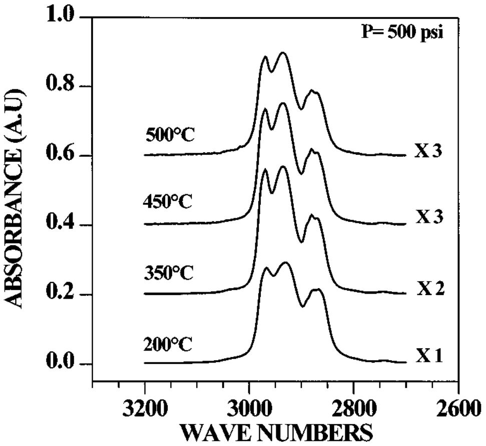

FIG. 6. *In situ* CIR-IR spectra of the stretching C–H modes of heptane flowing in a CIR-IR cell packed with promoted Octacat at subcritical (500 psi, 200°C) and supercritical (500 psi, 350°C and above) conditions. LHSV = 100 h^{-1}.

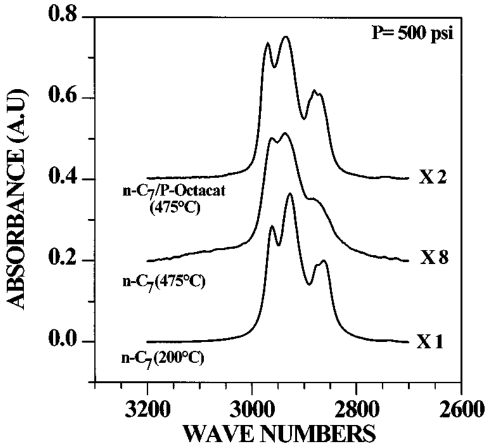

FIG. 7. *In Situ* CIR-IR spectra of subcritical (lower spectrum) and supercritical (middle spectrum) heptane flowing in an empty reactor cell and of supercritical heptane flowing in a reactor cell packed with promoted Octacat (upper spectrum). For all cases, heptane pressure, 500 psi, LHSV = 100 h^{-1}.

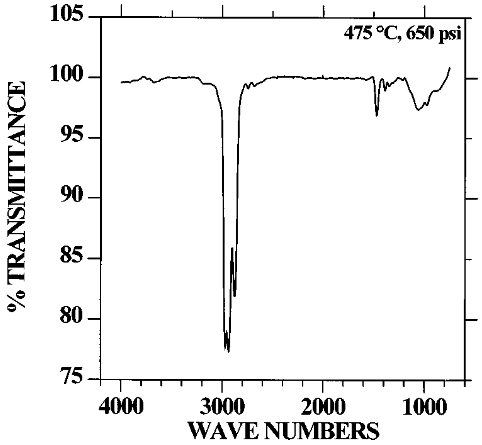

FIG. 8. *In situ* transmittance CIR-IR spectra at 475°C of promoted Octacat performing heptane cracking at supercritical conditions. Heptane pressure, 650 psi, LHSV = 160 h^{-1}.

observation was that the peaks of supercritical heptane within the catalyst were at least four times more intense than the corresponding peaks for supercritical pure heptane. This is surprising, since in the heptane/promoted-Octacat system, the total void space occupied by heptane (inside the particles and between the particles) is 0.62. This takes into account the fact that the sodalite cages in the USHY zeolite cannot be accessed by heptane. Therefore, the volume of heptane analyzed by IR in this system was lower than that of the heptane flowing in an empty cell. Additionally, the heptane/zeolite system did not show the large drop off in the intensity of the heptane C–H stretching modes at the critical temperature, indicating that heptane behaves like a liquid under these conditions.

Figure 7 compares the supercritical spectra of pure heptane, i.e., heptane in an empty cell, supercritical heptane over Octacat and subcritical pure heptane. The spectrum of supercritical heptane over the zeolite was intense, showed only the normal degree of infrared broadening and looked similar to the sharp spectrum of the subcritical liquid pure heptane. These facts suggest a liquid-like behavior of supercritical heptane within the zeolite pores, i.e., an increased heptane concentration within the zeolite pores. This is the first time that such an observation could be made to demonstrate the condensing effect of micropores on a hydrocarbon reactant under autogeneous catalytic conversion conditions. On the other hand, the heptane outside the zeolite micropores should be in the supercritical state. Because the supercritical state is characterized by less intense spectra, the heptane over zeolite spectrum must be the superposition of a dominant peak, corresponding to condensed heptane in the zeolite supercages, and of a weak peak, corresponding to the supercritical heptane in the small void spaces around the catalyst particles. Since the center of catalytic hydrocarbon cracking activity in H–Y zeolites is the supercage, this increased concentration effect under supercritical conditions could have an impact on the diffusivity and, therefore, on the selectivity of catalytic cracking products.

Temperature-Dependent CIR-IR Studies of a Commercial Catalytic Cracking H–Y Type Zeolite (Promoted Octacat)

Figure 8 presents the *in situ* transmittance CIR-IR spectrum of promoted Octacat (a commercial H–Y-type zeolite) performing catalytic cracking of supercritical heptane at 475°C and 650 psi. The quality of the spectrum at such high temperature should be again emphasized. This broad-range spectrum is of special importance for catalysis studies since it probes both the catalyst and the hydrocarbon reactant and products. The spectral region between 3800 and 3100 cm^{-1} corresponds to the stretching frequencies of the zeolite's hydroxyl groups and their interactions with the hydrocarbon reactant and products. The region between 3100 and 2600 cm^{-1} corresponds to the stretching C–H modes of the hydrocarbons while in the regimes between 1650 and 1600 cm^{-1} and 1550 and 1500 cm^{-1}, the stretching vibration modes of the C=C bonds of the olefinic and aromatic products, respectively, appear. Finally, between 1480 and 1360 cm^{-1}, the bending C–H modes of the hydrocarbons appear, while the spectral region from 1350 to 700 cm^{-1} corresponds to the stretching vibrations of the structural units of the zeolite (external linkages and internal tetrahedra).

Figure 9 presents the absorbance CIR-IR spectral region between 1500 and 700 cm^{-1} for the promoted Octacat at 150°C. For comparison, the spectra of an H–Y zeolite and kaolin clay are also shown in this figure. All these spectra were recorded under flowing nitrogen at 500 psi. According to Flanigen *et al.* (23) and Scherzer *et al.* (24),

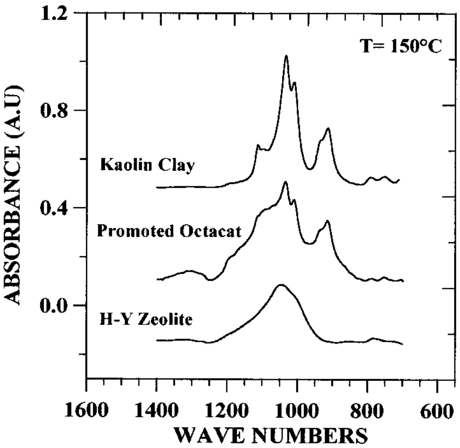

FIG. 9. *In situ* absorbance CIR-IR spectra of promoted Octacat, kaolin clay, and H–Y zeolite at 150°C. This spectral region corresponds to the stretching vibrations of the zeolite's structural units. All spectra were collected under flowing N_2 at 500 psi.

the strong spectral bands between 1110 and 900 cm^{-1} correspond to the asymmetric stretching modes of the internal SiO_4 and AlO_4 tetrahedra in the catalyst (23, 24). As this figure demonstrates, the peaks at 1105, 940, and 920 cm^{-1} originate from the kaolinite clay in the promoted Octacat. The spectral shoulders at 1200 and 1160 cm^{-1} correspond to the asymmetric stretching vibrations of the external linkages between the SiO_4 and AlO_4 internal tetrahedra, which are structure sensitive (23, 24). Finally, the weak spectral bands at 790 and 745 cm^{-1} were assigned to the symmetric stretching vibrations of the external linkages and the internal tetrahedra, respectively (24).

The spectra in Fig. 10 demonstrates the ability of the CIR technique to obtain high-quality spectra of the catalytically important acid sites of the zeolite at high temperatures. The various kinds of hydroxyl groups were identified and analyzed. The strong peak at 3749 cm^{-1} corresponds to the terminal silanol (Si–OH) groups (25–27). The dominant peak around 3680 cm^{-1} and the peak shoulder at 3650 cm^{-1} were assigned to physically adsorbed water molecules, bound through the oxygen atom to the Na^+ and other larger cations, respectively, in the kaolinite clay (27–29). The major band at 3626 cm^{-1} corresponds to the stretching vibration of the strongly acidic "bridged" (Si–OH–Al) hydroxyl groups (Brønsted acid sites), located in the supercages of the Y-type zeolite [25–32]. As Fig. 10 illustrates, acid sites from the kaolin clay also contribute to this band. Another weak band was also observed around 3600 cm^{-1} in the IR spectra at high temperatures (450°C), but its presence could only be revealed by the second derivative of the spectrum at lower temperatures. This band corresponds to the "superacidic sites" (33–36) in the ultrastable HY-type zeolite, which are formed from the perturbation of the hydroxyl groups in the supercages by the presence of nonframework aluminum (Lewis sites), generated from the dealumination process. The weak and broad peak around 3540 cm^{-1} corresponds to the stretching vibration mode of the hydroxyl groups located in the small sodalite cages. In general, this band is very weak for dealuminated HY-type zeolites (25, 33). Finally, the broad spectral bands between 3500 and 3100 cm^{-1} at 150°C, whose intensity dramatically decreased at higher temperatures, is assigned to strongly adsorbed water in the zeolite micropores and possibly to clustered silanol groups, i.e., structural hydrogen-bonded hydroxyl groups in the H–Y zeolite. Clustered silanol functionalities have been reported in the literature for H-ZSM-5 (37, 38).

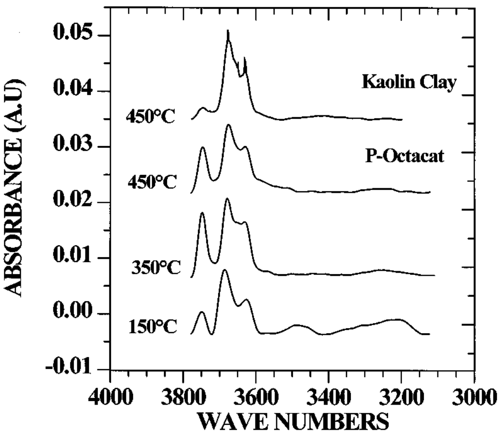

FIG. 10. Temperature-dependent CIR-IR hydroxyl adsorption spectra for promoted Octacat (number of data points used in smoothing algorithm, 17). All spectra were collected under flowing N_2 at 500 psi.

In Situ CIR-IR Analysis of Interactions of Heptane with Zeolite Hydroxyl Groups at both High Temperatures and Pressures

The interactions of heptane with the functional catalytic hydroxyl groups were monitored *in situ* during subcritical and supercritical catalytic cracking at 475°C. The spectra shown in Fig. 11 correspond to steady-state reaction conditions (heptane time on stream, 240 and 260 min, respectively). For comparison, the spectrum of pure catalyst collected at this temperature and pressure under flowing nitrogen is also presented in this figure. Dramatic changes occurred in the zeolite hydroxyl spectral region during heptane cracking. Curve fitting results showed that at subcritical conditions (200 psi), 75% of the terminal silanols and 60% of the Brønsted acid sites disappeared from the spectrum. Since coke formation accounts for the consumption of some of the catalyst's active sites, the CIR-IR results suggest coke formation in the supercages and silanols on the external surface of the catalyst. In addition, multiple new bands appeared in the spectra between 3500 and 3100 cm^{-1}. According to Makarova *et al.* (25), the bands between 3500 and 3300 cm^{-1} were assigned to the interactions of the catalyst hydroxyl groups with paraffins, i.e., heptane and heptane

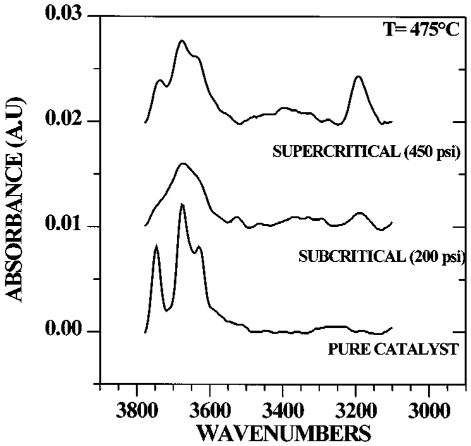

FIG. 11. Hydroxyl spectral region for promoted Octacat performing heptane cracking at 475°C, at subcritical (200 psi) and supercritical (450 psi) conditions (number of data points used in smoothing algorithm, 17). Heptane time-on-stream, 240 min for subcritical and 260 min for supercritical conditions. Heptane residence time, 0.50 sec.

cracking products, while the peaks slightly below 3300 cm^{-1} correspond to the interactions of the hydroxyl groups with olefinic products (25).

Increasing the pressure from subcritical (200 psi) to supercritical (450 psi) resulted in an increase in the concentration of the terminal silanols and Brønsted acid sites. At these conditions, the fresh catalyst has only lost 40% of the terminal silanols and 33% of the Brønsted acid sites. The heptane flow rate was adjusted in order to obtain the same heptane residence time (0.50 sec) for both pressures. The increase in the concentrations of the acid sites was accompanied by a large increase in the intensity of all the peaks between 3500 and 3100 cm^{-1} while the heptane conversion jumped from 17 to 23% under supercritical cracking conditions. The above observations suggest that supercritical heptane dissolves part of the coke that covers the acid sites of the catalyst and clogs the zeolite micropore openings, resulting in a partial regenation of the deactivated catalyst. This conclusion is consistent with detailed kinetic measurements and solubilization studies of phenanthrene (an aromatic hydrocarbon with three benzene rings used to simulate carbonaceous deposits) in a wide variety of supercritical hydrocarbons, which will be reported later in separate publications.

CONCLUSIONS

The *in situ* cylindrical reflectance infrared technique (CIR-IR) that was developed in this study enables the acquisition of high-quality spectra for the first time at both high temperatures and high pressures (temperatures up to 500°C and 1000 psi pressure (1 psi = 6850 Pa)). Therefore, *in situ* analysis of heterogeneous catalytic processes, like supercritical fuel cracking, can be quantitatively accomplished with this technique.

In situ observations of the molecular thermal transitions that heptane undergoes in the supercritical regime demonstrated an alteration of the IR absorption frequency of the C–H bonds.

In situ CIR-IR results demonstrated an increased heptane concentration within the pores of a commercial catalytic cracking Y-type zeolite (promoted Octacat) during cracking at supercritical conditions.

In situ CIR-IR studies of heptane catalytic cracking at 475°C and at subcritical and supercritical conditions showed that: (i) a significant number of Brønsted acid sites and terminal silanols are consumed during catalytic cracking, (ii) new spectral bands appear between 3500 and 3100 cm^{-1}, corresponding to the interactions of the acid sites with the reactant and products (paraffins and olefins), and (iii) acid sites regained a significant percentage of their initial concentrations during supercritical cracking, indicating that the catalyst starts recovering its activity under these process conditions.

ACKNOWLEDGMENTS

The Air Force Office of Scientific Research is gratefully acknowledged for financial support of this study under Grant Contract Number AFOSR G: F49620-93-1-0204. The authors also acknowledge United Technologies for their collaboration and helpful discussions.

REFERENCES

1. Fenstermacher, J. M., B.S. thesis, Worcester Polytechnic Institute, 1987.
2. Mireballa, F. M., and Harrick, N. J., "Internal Reflection Spectroscopy: Review and Supplement." Dekker, New York, 1985.
3. Harrick, N. J., *Phys. Rev. Lett.* **4**, 225 (1960).
4. Harrick, N. J., *J. Phys. Chem.* **64**, 1110 (1960).
5. Fahrenfort, J., *Spectrochim. Acta,* 698 (1962).
6. Wilks, P. A., *Ind. Res. Dev.* **Sept.**, 132 (1982).
7. Sting, D., and Wilks, P. A., "Scan Time." Barnes Analytical Spectra Tech., Stanford, CN, **2**, 1 (1982).
8. Alemdaroglu, N. Y., Penninger, J. L. M., and Oltay, E., *J. Mol. Catal.* 1 (1967).
9. Rigby, W., Whyman, R., and Wilding, K., *J. Phys. Sci. Instrum.* **2**, 572 (1978).
10. King, R. B., King, A. D., Ifbal, M. Z., and Frazier, C. C., *J. Am. Chem. Soc.* **100**, 1687 (1978).
11. Vidal, J. L., and Walker, W. E., *Inorg. Chem.* **19**, 896 (1980).
12. Moser, W. R., Cnossen, J. E., Wang, A. W., and Krouse, S. A., *J. Catal.* **95**, 21 (1985).
13. Moser, W. R., Chaing, J. C., and Cnossen, J. E., "Advances in Materials Characterization II" (R. L. Synder Condrate and P. P. Johnson, Eds.), Plenum, New York, 1985.
14. Moser, W. R., Papile, C. J., Brannon, D. A., Duwell, R. A., and Weininger, S. J., *J. Mol. Catal.* **41**, 271 (1987).
15. Moser, W. R., Papile, C. J., and Weininger, S. J., *J. Mol. Catal.* **41**, 293 (1987).
16. Moser, W. R., Wang, A. W., and Kildahl, N. K., *J. Am. Chem. Soc.* **110**, 2816 (1988).
17. Moser, W. R., Berard, J. R., Melling, P. J., and Burger, R. J., *Appl. Spectrosc.* **46(7)**, 1105 (1992).

18. Moser, W. R., *Adv. Chem. Ser.* **230**, 3 (1992).
19. Yokoyama, C., Kamo, Y., Takahashi, M., Ohtaka, K., and Takahashi, S., *Rev. Sci. Instrum.* **6415**, 1369 (1993).
20. Jolly, S., Saussey, J., and Lavelley, J. C., *J. Mol. Catal.* **86**, 401 (1994).
21. Brennecke, J. F., Tomasko, D. L., Peshkin, J., and Eckert, C. A., *Ind. Eng. Chem. Res.* **29**(8), 1681 (1990).
22. Dardas, Z., Süer, M. G., Ma, Y. H., and Moser, W. R., "Proceedings, Catalysis Society of New England, Dec. 1994."
23. Flanigen, E. M., Khatami, H., and Szymanski, H., *Adv. Chem. Ser.* **101**, 201 (1971).
24. Scherzer, J., and Ben, J. L., *J. Catal.* **28**, 101 (1973).
25. Makarova, M. A., and Dwyer, J., *J. Phys. Chem.* **97**, 6337 (1993).
26. Lohse, U., Loffler, E., Hunger, M., Stockner, J., and Patzelova, V., *Zeolites* **7**, 11 (1987).
27. Fritz, P. O., and Lundsford, J. H., *J. Catal.* **118**, 85 (1989).
28. Ward, J. W., *ACS Monogr.* **171**, 119 (1976).
29. Zhandov, S. P., Kiselew, A. W., Lygin, V. I., and Titova, T. J., *Russ. J. Phys. Chem.* **38**, 1299 (1964).
30. Dombrowski, D., Hoffman, J., and Fruwert, J., *J. Chem. Soc. Faraday Trans. 1* **81**, 2257 (1985).
31. Dwyer, J., Dewing, J., Thompson, N. E., O'Malley, P. J., and Karim, K. J., *Chem. Soc. Chem. Commun.,* 843 (1989).
32. Dwyer, J., Karim, K., Kayali, W., Milward, D., and O'Malley, P. J., *J. Chem. Soc. Chem. Commun.,* 594 (1988).
33. Mirodatos, C., and Bartomeuf, D., *J. Chem. Soc. Chem. Commun.,* 39 (1981).
34. Jacobs, P. A., and Uytterhoeven, J. B., *J. Chem. Soc. Faraday Trans. 1* **2**, 373 (1973).
35. Corma, A., Fornes, V., Perz-Pariente, J., Sastre, E., Martens, J. A., and Jacobs, P. A., *ACS Symp. Series* **368**, 555 (1988).
36. Chambellan, A., Chevran, T., Khabtov, S., Marzin, M., and Lavelley, J. C., *Zeolites* **12**, 306 (1992).
37. Moser, W. R., Chaing, C. C., and Thompson, R. W., *J. Catal.* **115**, 532 (1989).
38. Peri, J. B., "Proceedings, 5th International Congress on Catalysis, Palm Beach, 1972" (J. Hightower, Ed.), p. 329, Elseveir, New York, 1973.